Available online at www.sciencedirect.com
ScienceDirect
International Journal of Thermal Sciences 46 (2007) 848–855
International Journal of Thermal Sciences
www.elsevier.com/locate/ijts

Lattice Boltzmann modeling of the effective thermal conductivity for fibrous materials

Moran Wang [a], Jihuan He [b,c], Jianyong Yu [b], Ning Pan [a,b,*]

[a] *Division of Textiles and Clothing, Department of Biological & Agricultural Engineering, University of California, Davis, CA 95616, USA*
[b] *Center of Physics of Fibrous Soft Matters, Donghua University, Shanghai 200051, China*
[c] *College of Science, Donghua University, Shanghai 200051, China*

Received 29 September 2006; received in revised form 11 November 2006; accepted 12 November 2006

Available online 12 December 2006

Abstract

This paper presents a full set of numerical methods for predicting the effective thermal conductivity of natural fibrous materials accurately, which includes a random generation-growth method for generating micro morphology of natural fibrous materials based on existing statistical macroscopic geometrical characteristics and a highly efficient lattice Boltzmann algorithm for solving the energy transport equations through the fibrous material with the multiphase conjugate heat transfer effect considered. Using the present method, the effective thermal conductivity of random fibrous materials is analyzed for different parameters. The simulation results indicate that the fiber orientation angle limit will cause the material effective thermal conductivity to be anisotropic and a smaller orientation angle leads to a stronger anisotropy. The effective thermal conductivity of fibrous material increases with the fiber length and approach a stable value when the fiber tends to be infinite long. The effective thermal conductivity increases with the porosity of material at a super-linear rate and differs for different fiber location distribution functions.

Keywords: Effective thermal conductivity; Natural fibrous material; Statistical modeling; Lattice Boltzmann method

1. Introduction

Porous fibrous composites have many other important applications than those in textile engineering because of their ease of fabrication, relatively low cost and superior mechanical and thermal properties [1–5]. For example, the combination of reinforcement with high thermal conductivity embedded in a resin matrix with low thermal conductivity is desirable to replacing metal materials to dissipate the heat flux for electronic packaging components [2]. Very recently, the scanning electron micrographs of the carbon paper based porous transport layer (PTL) have shown that the microstructure in PTL has strongly fibrous nature but not the granular porous media as expected before [6]. Thus the heat and mass transportation characteristics through the PTL should be reconsidered for accurate predictions.

Generally speaking, thermal properties of a fibrous material depend on: (i) thermal properties of each phase (fiber and air), (ii) fiber volume fraction, and (iii) fiber size, orientation and mass distribution. A number of analytical models have been proposed to predict the thermal conductivity of short fiber composites [2,7–11], however most of which only involve the influences of factor (i) and (ii). Recently Fu and Mai [12] have introduced the effects of the fiber length distribution and orientation distribution into the analytical model through the laminate analogy approach (LAA) [13] for predicting the effective thermal conductivity of short-fiber-reinforced polymer composites. It was observed that the thermal conductivity of the composite increases with mean fiber length but decreases with mean fiber orientation angle with respect to the measured direction. This model is more suitable for dilute short-fiber composite because it becomes very complicated when the inter-fiber connections are in large number. To our knowledge, there is no effective analytical method yet that can predict, with acceptable accuracy, the effective thermal conductivity of fibrous materials while taking into account the effects of material structure. Ow-

* Corresponding author.
E-mail addresses: mmwang@ucdavis.edu (M. Wang), npan@ucdavis.edu (N. Pan).

1290-0729/$ – see front matter
doi:10.1016/j.ijthermalsci.2006.11.006

ing to the rapid development of computer and computational techniques in the past a couple of decades, numerical modeling methods have provided an alternative in dealing with the properties of fibrous materials with complex geometries. To achieve a reliable prediction, one needs to work on two aspects: a full description of the structural details of fibrous materials, and an efficient numerical method for the solution of energy equations through the fibrous structures.

By and large, it is extremely difficult, if not impossible, to completely describe the internal structure of a fibrous medium due to its complex and stochastic nature. One often can only acquire the statistic-based average information such as the mean porosity, the mean fiber contacting length and the orientation range. Nonetheless using computers there have been some attempts to re-produce the statistic–stochastic characteristics of fibrous composite materials through several different methods [9,12,14–19]. For instance, recently the tessellation-based Voronoi cells have been extracted for generating the fiber distribution [9]; Torquato et al. [20–22] simulated disordered arrangements of composite media by using the statistical means and high-order correlation functions; Eichhorn and Sampson [15] and Scharcanski et al. [14] investigated the stochastic characteristics of the internal structure of fibrous materials and suggested relationships between the statistical mean porosity and the micro-structural characteristics which could be helpful for fibrous structure generation.

Next, to predict the effective thermal conductivity of a fibrous medium with given structure, the energy equations must be solved through the multiphase structure. The structural complexities bring two challenges when the governing equations are to be solved by conventional numerical tools such as the finite difference [23,24] and finite element methods [9]. The first is the constraint on inter-phase conjugate heat transfer: for steady pure heat conduction through multiple phases, temperature and heat flux continuities have to be ensured at the interfaces only if the contact thermal resistance is negligible [25–29] when solving the governing equations, thus demanding extremely high computational resources for a fibrous medium with innumerable interfaces in the structure. The second is the requirement of grid refinement for complex structures: the accuracy of a conventional numerical method is strongly dependent on the grid size so an extra fine grid is needed whenever the transport process is complex in physics and/or in geometry. When dealing with such multi-phase conjugate heat transfer problems in fibrous materials with complex geometries, this requirement will confine the computational domain into a very limited area. To overcome these two difficulties, Wang et al. [30] proposed a much more efficient thermal lattice Boltzmann algorithm to solve the energy equations in multiple phases where the continuity constraints are self-satisfied owing to this new approach and much less grid number is required for the same accuracy. The predictions agreed well with the experimental data for different structures [31].

The objective of this paper is to develop a robust computer simulation model for predicting the effective thermal conductivity of fibrous materials reflecting the influences of the structural characteristics. The model will enable conduction of parametric simulations to investigate the effects of various related factors on the effective thermal conductivity. The model, once completed, should provide a powerful tool for various fibrous product designs and thermal performance optimizations.

In the following sections, we first develop a method for generating stochastic microstructures based on macroscopic statistical information, and then introduce the efficient lattice Boltzmann approach for solving the energy equations through a multiphase structure. Next, we present two-dimensional (2D) results of mesoscopic simulations addressing the influence of fiber orientation angle, fiber length, mean porosity, and the fiber location distribution function on the effective thermal conductivity.

2. Numerical methods

The numerical methods introduced in this section include a random generation-growth algorithm for constructing the internal structure of fibrous materials and a lattice Boltzmann model for solving the energy equations through the materials.

2.1. Structure generation of fibrous materials

To investigate the influences of the internal structure, one needs first a detailed description of the structure. However, given the stochastic nature of the structure, it would be extremely complex to derive such an analytical description either theoretically or experimentally. Thus we propose a stochastic generation-growth method to produce the fibrous material structures based on the given fiber properties and distribution requirements.

Consider a two-dimensional and two-phase (fiber/air) fibrous material, whose internal structure is shown as Fig. 1 under SEM [32]. We assume each fiber is represented by a straight line with given diameter d and length l, and located by its core position and orientation angle θ, as illustrated in Fig. 2. The structure generation process is conducted as follows:

- (i) randomly locate the fiber cores based on a core distribution probability, c_d, and the core position distribution function, F. The core distribution probability c_d is defined as the probability of a point to become a core of fiber. The value of c_d is strongly relative to the fiber number density. The core position distribution function F could be a uniform, a normal or any other distribution function of position (x, y);
- (ii) randomly assign an orientation angle θ to each fiber core, and if the value of angle limit is given other than $0 \sim \pi$, the orientation angle of a fiber can be any value within $[-\theta_{\text{lim}}, \theta_{\text{lim}}]$;
- (iii) grow fibers from the cores along both directions of the orientation θ for length and grow the fiber sections for width;
- (iv) stop growth once fiber dimensions, d and l, reach the specified values, or the porosity attains the given level ε.

Thus there are six parameters, c_d, F, θ_{lim}, d, l, and ε controlling the resulting structure, yet the porosity, ε, is dependent on

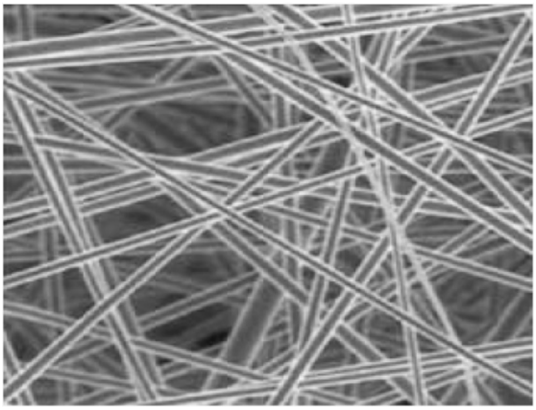

Fig. 1. Internal structure of fibrous material under SEM [32].

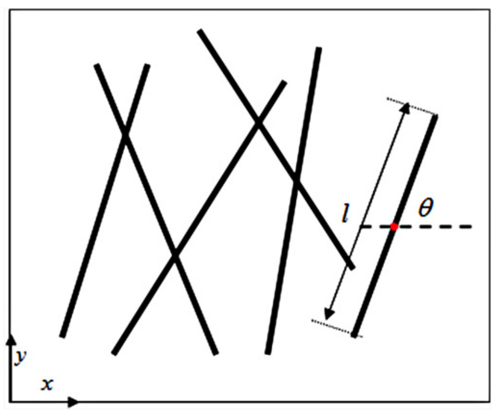

Fig. 2. Schematic illustration of grown fibers and parameters.

the other five parameters, strongly by c_d, d, and l, and slightly by F and $\theta_{\lim}$ which actually influence the inter-fiber contacts.

Fig. 3 shows five examples of generated morphologies in 200×200 grids for various values of parameters. The white represents the fiber and the dark the gas or other fluids. Comparisons between (a) and (c), and (b) and (d) indicate that both c_d and l have strong influence on the porosity of the materials. The anisotropy will change by the values of both $\theta_{\lim}$ and F from comparing between (a) and (b), and (d) and (e).

2.2. Statistical solution of energy equations—the Lattice Boltzmann Model (LBM)

To calculate the effective thermal conductivity of fibrous materials, we have to solve the energy equations for the temperature and heat flux fields. Consider a pure thermal conduction through a fibrous structure with the following assumptions: two phases only and no phase change; no convection and radiation—the former is true when the pore sizes are small and the external flow velocity is low. When the contact thermal resistance between fibers is negligible, the energy equations under such assumptions for thermal conduction through fibrous structures without heat sources are

$$(\rho c_p)_f\left(\frac{\partial T}{\partial t}\right)=k_f\nabla^2 T \tag{1}$$

$$(\rho c_p)_g\left(\frac{\partial T}{\partial t}\right)=k_g\nabla^2 T \tag{2}$$

with the continuity constrains at the inter-phase surfaces

$$T_{f,\text{int}}=T_{g,\text{int}} \tag{3}$$

$$k_f\frac{\partial T}{\partial n}\bigg|_{f,\text{int}}=k_g\frac{\partial T}{\partial n}\bigg|_{g,\text{int}} \tag{4}$$

where subscript f represents the fiber and g the gas, and int the interfaces; T is temperature, ρ is density, k is the thermal conductivity, and c_p is the specific heat capacity. Eqs. (1)–(4) describe a classical case of the multiphase conjugate heat transfer problem [33]. At the fiber/air interfaces, both the temperature and heat flux continuities have to be satisfied. As stated above, this interface constraint increases the computational costs tremendously when using the conventional numerical methods. Moreover, since there are huge numbers of such interfaces in fibrous media, this further pushes the computational cost into prohibitive.

Recently, the lattice Boltzmann method (LBM) has been developed to solve effectively the fluid–solid conjugate heat transfer [30], which is intrinsically a mesoscopic approach based on the evolution of statistical distribution on lattices [34,35]. Due to its easy implementations of multiple interparticle interactions and complex geometry boundary conditions [36–38], the LBM has gained several successes in predicting the effective thermal conductivities of conventional porous media [31,39]. We thus propose to adopt the highly efficient LBM approach, which can easily tackle the multiple component/phase interactions and complex structural boundary conditions, while being auto-conservative. Furthermore, because of the requirement of temperature and heat flux continuities at phase interfaces, the volume thermal capacities (ρc_p) at different phases have to be maintained as the same [33]; therefore the conjugate heat problem between different phases is thus solved. Here we follow our previous work using the lattice Boltzmann algorithm for the fluid-solid conjugate heat transfer problem [30], and believe this is the first such attempt on fibrous materials.

For the pure thermal conduction in fibrous materials governed by Eqs. (1)–(4), the temperature evolution equation for a two-dimensional nine-speed (D2Q9) LBM in both fiber and gas phases can be generally given as [30],

$$g_\alpha(\mathbf{r}+\mathbf{e}_\alpha\delta_t,t+\delta_t)-g_\alpha(\mathbf{r},t)=-\frac{1}{\tau}\left[g_\alpha(\mathbf{r},t)-g_\alpha^{\text{eq}}(\mathbf{r},t)\right] \tag{5}$$

where $\mathbf{r}$ is the location vector, t the real time, δ_t the time step, g^{eq} the equilibrium distribution of the evolution variable g_α

$$g_\alpha^{\text{eq}}=\begin{cases}0 & \alpha=0\\ \frac{1}{6}T & \alpha=1,2,3,4\\ \frac{1}{12}T & \alpha=5,6,7,8\end{cases} \tag{6}$$

$\mathbf{e}_\alpha$ is the discrete velocity

$$\mathbf{e}_\alpha=\begin{cases}(0,0) & \alpha=0\\ (\cos\theta_\alpha,\sin\theta_\alpha)c & \theta_\alpha=(\alpha-1)\pi/2\\ & \alpha=1,2,3,4\\ \sqrt{2}(\cos\theta_\alpha,\sin\theta_\alpha)c & \theta_\alpha=(\alpha-5)\pi/2+\pi/4\\ & \alpha=5,6,7,8\end{cases} \tag{7}$$

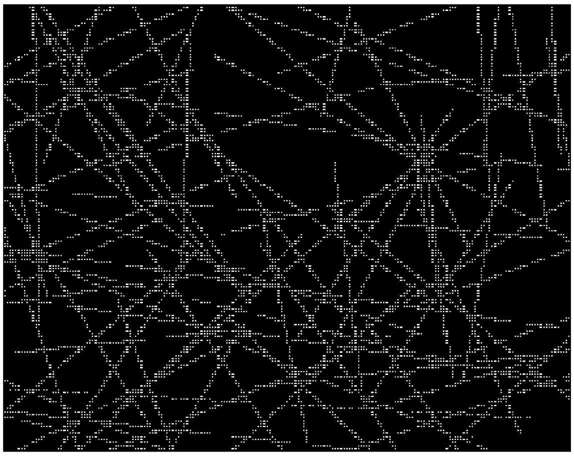

(a) c_d =0.0025, d=δ_x, l =100 δ_x, $\theta_{\text{lim}} = \pi/2$,

Uniform distribution

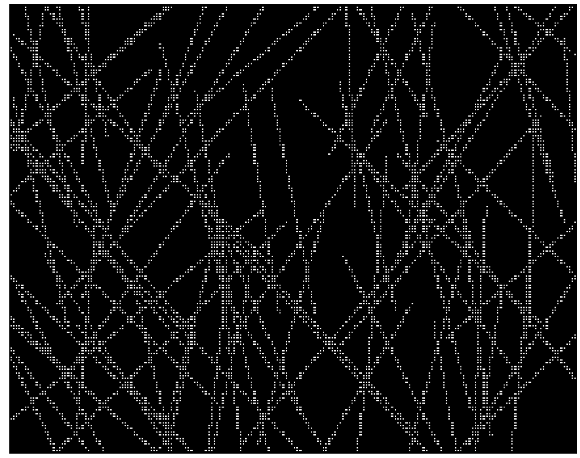

(b) c_d =0.0025, d=δ_x, l =100 δ_x, $\theta_{\text{lim}} = \pi/4$,

Uniform distribution

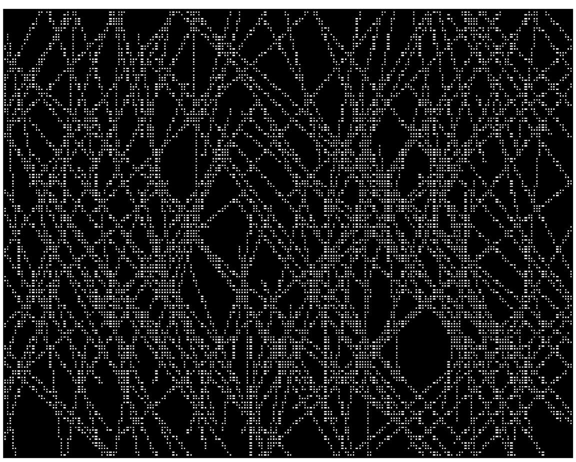

(c) c_d =0.005, d=δ_x, l =100 δ_x, $\theta_{\text{lim}} = \pi/4$,

Uniform distribution

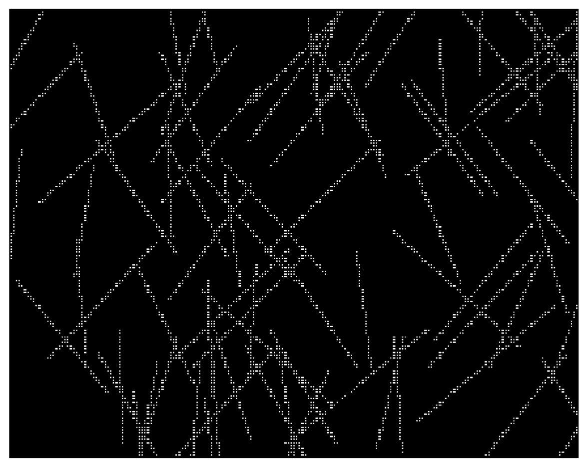

(d) c_d =0.0025, d=δ_x, l =50 δ_x, $\theta_{\text{lim}} = \pi/4$,

Uniform distribution

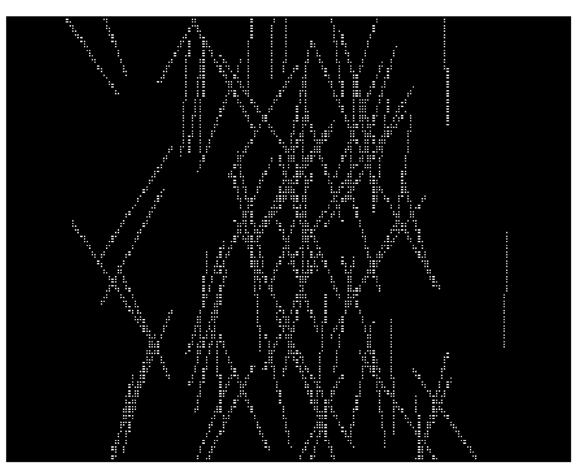

(e) c_d =0.0025, d=δ_x, l =50 δ_x, $\theta_{\text{lim}} = \pi/4$,

Normal distribution and symmetric to axis x =100

Fig. 3. Generated fibrous materials with different parameters.

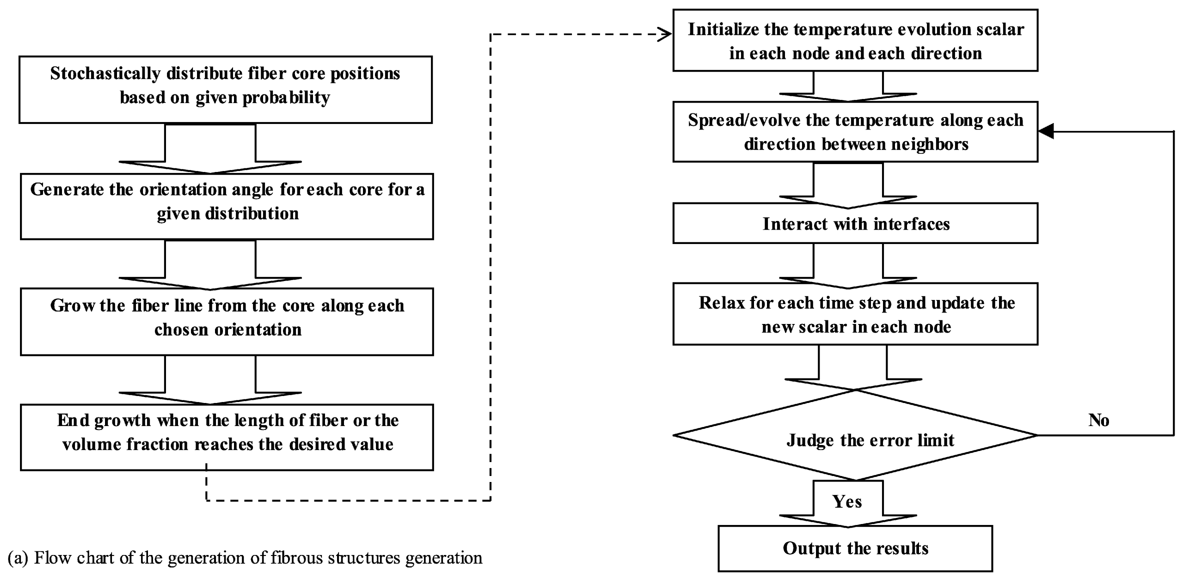

(a) Flow chart of the generation of fibrous structures generation

(b) Flow chart of the Lattice Boltzmann model

Fig. 4. Flow charts of the present algorithms.

and τ the dimensionless relaxation time for each phase which is determined by the thermal conductivity of each phase,

$$\tau_f = \frac{3}{2}\frac{k_f}{(\rho c_p)_f \cdot c^2\delta_t} + 0.5 \tag{8}$$

and

$$\tau_g = \frac{3}{2}\frac{k_g}{(\rho c_p)_g \cdot c^2\delta_t} + 0.5 \tag{9}$$

where we have to set $(\rho c_p)_f$ equal to $(\rho c_p)_g$ in the simulations to assure the continuity at the interfaces [33]; c is the *pseudo* sound speed, defined as δ_x/δ_t where δ_x is the lattice constant (i.e., the grid size), whose value can take any positive value theoretically only to insure the values of τ within (0.5, 2) [30].

The temperature and the heat flux can be then calculated by [30,40]

$$T = \sum_\alpha g_\alpha \tag{10}$$

$$q = \left(\sum_\alpha \mathbf{e}_\alpha g_\alpha\right)\frac{\tau - 0.5}{\tau} \tag{11}$$

For the isothermal boundary treatment, we follow the bounce-back rule of the non-equilibrium distribution proposed by Zou and He [41]

$$g_\alpha - g_\alpha^{\mathrm{eq}} = -\left(g_\beta - g_\beta^{\mathrm{eq}}\right) \tag{12}$$

where α and β represent opposite directions, and the equilibrium distribution can be calculated by the local boundary temperature.

For the insulated boundary, a specula reflection treatment is implemented in this paper to avoid energy leak along the surfaces. After the temperature field is solved, the effective thermal conductivity, k_{eff}, can be determined:

$$k_{\mathrm{eff}} = \frac{L \cdot \int q \cdot dA}{\Delta T \int dA} \tag{13}$$

where q is the steady heat flux through the media cross section area dA between the temperature difference ΔT with a distance L. All of these parameters can be theoretically determined, and thus there are no empirical factors existed in the model.

3. Results and discussion

The suggested approaches include a stochastic generation-growth algorithm for producing the practical structures of fibrous materials, and a lattice Boltzmann model for solving the energy equations through the materials. The flowcharts corresponding to the two parts are shown in Fig. 4(a) and (b).

In this paper, we focus on the effects of fiber orientation angle limit, θ_{lim}, fiber length, l, fiber volume fraction $(1-\varepsilon)$ or porosity, ε, and the fiber location distribution function F on the effective thermal conductivity of fibrous materials by assuming the fiber width maintains constant. In the following simulations, 200×200 grids are employed for the generations of two-dimensional fibrous networks where the grid size is $\delta_x = 15$ μm. The thermal conductivities of fiber and gas are set to 0.5 and 0.025 $\mathrm{W\,m^{-1}\,K^{-1}}$ respectively. For anisotropic cases, if only the effective thermal conductivities at x-direction are concerned, we will set the left ($x=0$) and right ($x=200$) boundaries to be of Dirichlet/isothermal type and the up ($y=200$) and down ($y=0$) boundaries to be insulated. If the y-directional ones are concerned, the up and down boundaries will be isothermal and the left and right will be insulated. We then set the temperatures at the two isothermal boundaries to 100 and 200 K respectively to form a temperature gradient.

Since the stochastic factors have been introduced during the material structure generation process, the calculated effective thermal conductivity will not be identical in every trial, but fluctuate around an average value. In following work therefore, we

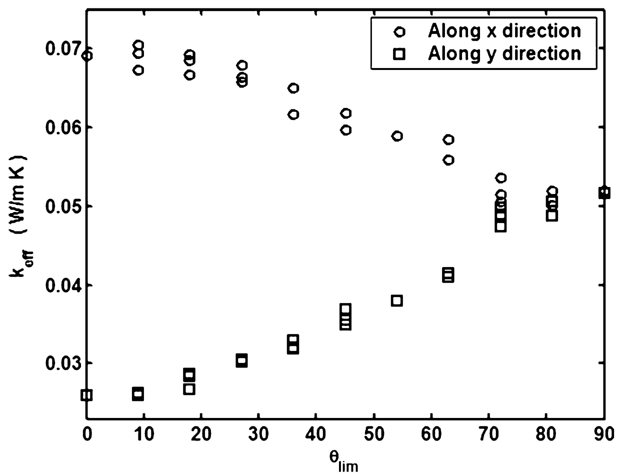

Fig. 5. The effective thermal conductivity versus the fiber orientation angle limit. The other parameters are $c_d = 0.0025$, $d = \delta_x$, $l = 50\delta_x$, and the fiber locations are follow a uniform distribution function.

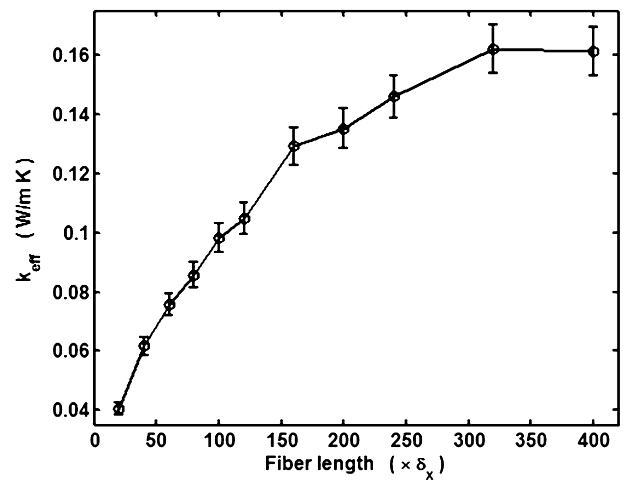

Fig. 6. The x-directional effective thermal conductivity versus the fiber length l. The other parameters are $c_d = 0.0025$, $d = \delta_x$, $\theta_{\rm lim} = \pi/8$, and the fiber locations follows a uniform distribution function.

perform five simulations for each case and take the averaged value as the final result.

Fig. 5 shows the calculated effective thermal conductivities as functions of the fibers orientation angle limit. The case $\theta_{\rm lim} = 0$ means all the fibers are parallel to the x axis, which leads to the strongest anisotropy. On the contrary, an isotropy is reached at the case $\theta_{\rm lim} = \pi/2$ where all the fibers have equal probability to lie in any direction. In Fig. 5, the circles represent the effective thermal conductivities in x direction and the squares in y direction. The two effective thermal conductivity values differ by over 2.5 times at $\theta_{\rm lim} = 0$ and almost equal to each other at $\theta_{\rm lim} = \pi/2$. We performed 2 or 3 calculations for each $\theta_{\rm lim}$ value. The random characteristics of microscopic positions and connections of fibers made the resulted effective thermal conductivity fluctuate around an average value for same macroscopic parameters. The uncertainty of results is mainly dependent on the grid number used. For our cases, the maximum relative deviation from the average value is less than 10% and the averaged relative deviation is about 5% for the 200×200 grid.

Fig. 6 shows the effective thermal conductivity changing with the length l of fibers when other factors are fixed. Because the simulations are performed in a finite domain (200×200), a fiber by a length $l = 400\delta_x$ almost means infinite long to the domain. As a result, when the length approaches $400\delta_x$, the calculated effective thermal conductivity tends to level off. Either x-directional or y-directional results has the same shape of curve that rises sharply at short fiber length and slows down at long length, then stabilizes when the limit approaches the domain size: in the present simulation, that stable value is about $0.16\ \mathrm{W\,m^{-1}K^{-1}}$.

As mentioned before, the porosity of a fibrous material is dependent not only on the fiber distribution density (mainly controlled by the value of c_d), but also on the fiber shape and fiber–fiber contacts. Therefore the porosity could differ significantly even for the same value of c_d, especially at high level. In this work, we vary c_d from 0.001 to 0.01 when $\theta_{\rm lim} = \pi/4$, $l = 100\delta_x$, and the fiber locations are uniformly distributed. The

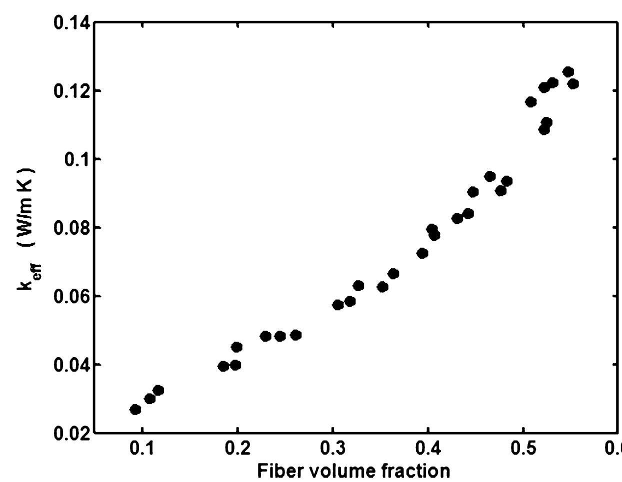

Fig. 7. The x-directional effective thermal conductivity versus the volume fraction of fibers. The other parameters are $\theta_{\rm lim} = \pi/4$, $d = \delta_x$, $l = 100\delta_x$, and uniform fiber location distribution.

x-directional effective thermal conductivity versus the porosity is provided in Fig. 7. The results indicate the effective thermal conductivity increases with the porosity at a near-linear rate, which is consistent with the experimental curves in the literature [42,43], for increasing fiber amount reduces air in the system which has higher thermal resistance when convection is negligible.

Finally, the effects of the fiber location distribution function (local fiber distribution uniformity) on the effective thermal conductivity are studied. Both a uniform and a normal distribution functions are compared, the differences in the structures generated are already shown in Fig. 3(d) and (e). It is clear that any non-uniform fiber location distribution function will lead the fibrous material to a greater anisotropy. Here we set the same parameters $c_d = 0.0025$, $l = 50\delta_x$ and $\theta_{\rm lim} = \pi/4$ for both distribution functions. The calculated x-directional and y-directional effective thermal conductivities are 0.0667 and 0.0278 $\mathrm{W\,m^{-1}\,K^{-1}}$ respectively for the uniform distribution case, and the corresponding values are 0.0599 and $0.0281\ \mathrm{W\,m^{-1}\,K^{-1}}$ for the normal distribution one. The results indicate the effective thermal conductivity changes due to the fiber orientation and fiber–fiber contacts changed by the different location distributions. Fibers are inherently anisotropic and this anisotropy will translate into the system anisotropy differently when fiber orientation changes and the condition $\theta_{\lim} = \pi/4$ also alters the otherwise x–y symmetry. The x-directional effective thermal conductivity for uniform distributed fibers ($0.0667\ \mathrm{W\,m^{-1}\,K^{-1}}$) is remarkably larger than that for normal distributed fibers ($0.0599\ \mathrm{W\,m^{-1}\,K^{-1}}$). Whereas the y-directional value for a uniform distribution is ($0.0278\ \mathrm{W\,m^{-1}\,K^{-1}}$) slightly smaller than that for a normal distribution ($0.0281\ \mathrm{W\,m^{-1}\,K^{-1}}$), statistically insignificant.

4. Conclusions

This paper presented a stochastic–statistic–mechanics scheme for modeling the effective thermal conductivity of fibrous materials, which includes a structure generation-growth method for analytically constructing a fibrous material based on given statistical macroscopic information, and a lattice Boltzmann algorithm for solving the energy transport equations through the fibrous material with the multiphase conjugate heat transfer effect considered.

Using the present method, the effective thermal conductivity of 2-dimensional fibrous networks is analyzed for different given parameters. The results indicate that the inherent fiber anisotropy will translate into the system anisotropy through different fiber orientations. The fiber orientation angle limit will also cause the material effective thermal conductivity to be anisotropic and a smaller angle limit leads to a greater anisotropy. Also, the fiber orientation angle range less than $0 \sim \pi/2$ will alters the otherwise x–y symmetry.

The effective thermal conductivity of fibrous material increases with the fiber length and approach a stable value when the fiber length is sufficiently long. The effective thermal conductivity increases with the porosity of material at a near-linear rate, for increasing fiber amount reduces the air in the system, which has higher thermal resistance when air convection is negligible. The effective thermal conductivity differs for different fiber location distribution functions (i.e. local fiber distribution uniformity) as well.

Acknowledgements

The authors would like to thank the grant support by the National Textile Center (NTC) M04-CD01.

References

[1] O. Jirsak, T. Gok, B. Ozipek, N. Pan, Comparison between a dynamic and a static methods for measurement of thermal conductive properties of textiles, Textile Research Journal 68 (1998) 47–56.

[2] M. Idicula, A. Boudenne, L. Umadevi, L. Ibos, Y. Candau, S. Thomas, Thermophysical properties of natural fibre reinforced polyester composites, Composites Science and Technology 66 (2006) 2719–2725.

[3] J.H. Wu, N. Pan, Grab and strip tensile strengths for woven fabrics: An experimental verification, Textile Research Journal 75 (11) (2005) 789–796.

[4] S.Y. Fu, B. Lauke, Fracture resistance of unfilled and calcite-particle-filled ABS composites reinforced by short glass fibers (SGF) under impact load, Composites Part A—Applied Science and Manufacturing 29 (5–6) (1998) 631–641.

[5] S.Y. Fu, B. Lauke, The fibre pull-out energy of misaligned short fibre composites, Journal of Materials Science 32 (8) (1997) 1985–1993.

[6] J.G. Pharoah, K. Karan, W. Sun, On effective transport coefficients in PEM fuel cell electrodes: Anisotropy of the porous transport layers, Journal of Power Sources 161 (1) (2006) 214–224.

[7] L.-W. Fan, Y.C. Hu, T. Tian, Z.T. Yu, The prediction of effective thermal conductivities perpendicular to the fibres of wood using a fractal model and an improved transient measurement technique, International Journal of Heat and Mass Transfer 49 (21–22) (2006) 4116–4123.

[8] Y.-M. Lee, R.-B. Yang, S.-S. Gau, A generalized self-consistent method for calculation of effective thermal conductivity of composites with interfacial contact conductance, International Communications in Heat and Mass Transfer 33 (2) (2006) 142–150.

[9] I.J. Turias, J.M. Gutierrez, P.L. Galindo, Modelling the effective thermal conductivity of an unidirectional composite by the use of artificial neural networks, Composites Science and Technology 65 (3–4) (2005) 609–619.

[10] P.G. Klemens, Thermal conductivity of fibre composites at low temperatures, Cryogenics 31 (4) (1991) 238–240.

[11] S.M. Grove, A model of transverse thermal conductivity in unidirectional fibre-reinforced composites, Composites Science and Technology 38 (3) (1990) 199–209.

[12] S.Y. Fu, Y.W. Mai, Thermal conductivity of misaligned short-fiber-reinforced polymer composites, Journal of Applied Polymer Science 88 (6) (2003) 1497–1505.

[13] S.Y. Fu, B. Lauke, The elastic modulus of misaligned short-fiber-reinforced polymers, Composites Science and Technology 58 (3–4) (1998) 389–400.

[14] J. Scharcanski, C.T.J. Dodson, R.T. Clarke, Simulating effects of fiber crimp, flocculation, density, and orientation on structure statistics of stochastic fiber networks, Simulation (2002) 389–395.

[15] S.J. Eichhorn, W.W. Sampson, Statistical geometry of pores and statistics of porous nanofibrous assemblies, Journal of the Royal Society Interface 2 (4) (2005) 309–318.

[16] R. Pyrz, Quantitative description of the microstructure of composites. Part I: Morphology of unidirectional composite systems, Composites Science and Technology 50 (2) (1994) 197–208.

[17] S. Ghosh, Z. Nowak, K. Lee, Quantitative characterization and modeling of composite microstructures by Voronoi cells, Acta Materialia 45 (6) (1997) 2215–2234.

[18] S. Ghosh, Z. Nowak, K. Lee, Tessellation-based computational methods for the characterization and analysis of heterogeneous microstructures, Composites Science and Technology 57 (9–10) (1997) 1187–1210.

[19] B. Bochenek, R. Pyrz, Reconstruction of random microstructures—a stochastic optimization problem, Computational Materials Science 31 (1–2) (2004) 93–112.

[20] L.V. Gibiansky, S. Torquato, New method to generate three-point bounds on effective properties of composites: Application to viscoelasticity, Journal of the Mechanics and Physics of Solids 46 (4) (1998) 749–783.

[21] S. Hyun, S. Torquato, Designing composite microstructures with targeted properties, Journal of Materials Research 16 (1) (2001) 280–285.

[22] S. Torquato, Modeling of physical properties of composite materials, International Journal of Solids and Structures 37 (1–2) (2000) 411–422.

[23] H.F. Zhang, X.S. Ge, H. Ye, Randomly mixed model for predicting the effective thermal conductivity of moist porous media, Journal of Physics D: Applied Physics 39 (1) (2006) 220–226.

[24] H.F. Zhang, X.S. Ge, H. Ye, Effectiveness of the heat conduction reinforcement of particle filled composites, Modelling and Simulation in Materials Science and Engineering 13 (3) (2005) 401–412.

[25] G.S. Springer, S.W. Tsai, Thermal conductivities of unidirectional materials, Journal of Composite Materials 1 (1967) 166–173.

[26] L.S. Han, A.A. Cosner, Effective thermal conductivities of fibrous composites, Journal of Heat Transfer 103 (1981) 387–392.

[27] D.P.H. Hasselman, K.Y. Donaldson, J.R. Thomas, Effective thermal conductivity of uniaxial composite with cylindrically orthotropic carbon fibers

and interfacial barrier, Journal of Composite Materials 27 (6) (1993) 637–644.
[28] A.C. Rodríguez, J.M.G. Cabeza, Effect of cylindrically orthotropic carbon fibers with transversely isotropic core on effective thermal conductivity of unidirectional composites, Journal of Composite Materials 33 (11) (1999) 984–1001.
[29] R. Pal, Porosity-dependence of effective mechanical properties of pore-solid composite materials, Journal of Composite Materials 39 (13) (2005) 1147–1158.
[30] J. Wang, M. Wang, Z. Li, A lattice Boltzmann algorithm for fluid–solid conjugate heat transfer, International Journal of Thermal Sciences (2007), in press, doi:10.1016/j.ijthermalsci.2006.04.012.
[31] M. Wang, J. Wang, N. Pan, S.Y. Chen, Mesoscopic predictions of the effective thermal conductivity for microscale random porous media, Physical Review E (2007), in press.
[32] L. Li, Y.-L. Hsieh, Ultra-fine polyelectrolyte fibers from electrospinning of poly(acrylic acid), Polymer 46 (14) (2005) 5133–5139.
[33] X. Chen, P. Han, A note on the solution of conjugate heat transfer problems using SIMPLE-like algorithms, International Journal of Heat and Fluid Flow 21 (4) (2000) 463–467.
[34] X. He, S. Chen, G.D. Doolen, A novel thermal model for the lattice Boltzmann method in incompressible limit, Journal of Computational Physics 146 (1) (1998) 282–300.
[35] S. Chen, G.D. Doolen, Lattice Boltzmann method for fluid flows, Annual Review of Fluid Mechanics 30 (1998) 329–364.
[36] Q.J. Kang, D.X. Zhang, P.C. Lichtner, I.N. Tsimpanogiannis, Lattice Boltzmann model for crystal growth from supersaturated solution, Geophysical Research Letters 31 (21) (2004) L21604.
[37] Q.J. Kang, D.X. Zhang, S.Y. Chen, Simulation of dissolution and precipitation in porous media, Journal of Geophysical Research—Solid Earth B 108 (10) (2003) 2505.
[38] Q.J. Kang, D.X. Zhang, S.Y. Chen, X.Y. He, Lattice Boltzmann simulation of chemical dissolution in porous media, Physical Review E 65 (3) (2002) 036318.
[39] M. Wang, J. Wang, N. Pan, S.Y. Chen, Three-dimensional effect of the effective thermal conductivity of porous media, Journal of Physics D: Applied Physics (2007), in press.
[40] A. D'Orazio, M. Corcione, G.P. Celata, Application to natural convection enclosed flows of a lattice Boltzmann BGK model coupled with a general purpose thermal boundary condition, International Journal of Thermal Sciences 43 (2004) 575–586.
[41] Q.S. Zou, X.Y. He, On pressure and velocity boundary conditions for the lattice Boltzmann BGK model, Physics of Fluids 9 (6) (1997) 1591–1598.
[42] A. Bouguerra, Temperature and moisture dependence on the thermal conductivity of wood-cement-based composite: Experimental and theoretical analysis, Journal of Physics D: Applied Physics 32 (21) (1999) 2797–2803.
[43] A. Bouguerra, A. Ledhem, J.P. Laurent, M.B. Diop, M. Queneudec, Thermal effusivity of two-phase wood cement-based composites, Journal of Physics D: Applied Physics 31 (17) (1998) 2184–2190.